Journal of Computer Methods in Civil Engineering
Volume 2, Issue 1, No. 2
Received 24 October 2022; Accepted 22 November 2022
Published online December 26 2022

Sanderman Publishing House

Numerical solution of dissimilar inclusion problem for square notch with small round corners in plane elasticity

Yizhou Chen
Division of Engineering Mechanics, Jiangsu University, Zhenjiang, P. R. China
E-mail : *chens@ujs.edu.cn*

Abstract. In this paper, the stress solution for a square notch with small round corners is studied. The square notch is composed of two portions, or the matrix and the inclusion. The elastic property of the inclusion portion is different to that of the matrix. Remote loading is applied. When the dissimilar inclusion is embedded in the matrix, the stress state in the inclusion will be changed significantly. The interface conditions along interface are formulated exactly. Complex variable function method is used to solve the problem. The complex potentials in the matrix and the inclusion are assumed in different structure. In the formulation, the number of the equations is larger than that of the unknowns. Therefore, the weight residue technique is used to solve the algebraic equation. The tangential, normal and shear stress components along the interface from the matrix and inclusion side are evaluated from the solution of the algebraic equation. In the computation, significant stress concentration has been found for the tangential stress component.

Keywords. Dissimiler inclusion, inhomogeneity, complex variable method, weight residue technique, stress concentration factor.

1. Introduction

The notch problem plays an important role in machine design, simple because the stress concentration happens at the small radius corner. The complex variable method is a powerful tool to solve the problem [1]. Many solutions for notch problem in plane elasticity were developed [2]. In old years, one could not complete the relevant computation for lacking of modern computer. Therefore, the previously obtained solutions in this field were not significant.

From the definition proposed in [3], inclusions can be categorized by into inhomogeneous inclusions, homogeneous inclusions and inhomogeneities. For a wide range of the inclusion problem, two survey papers were published [4, 5].

A solution is presented for determining the stresses in an infinite elastic plate containing a rectangular inclusion subjected to a uniform stress field [6]. The point matching method is used to find the final solution. A boundary integral equation approach was used to solve an infinite anisotropic elastic inclusion problem subjected to remote loading [7]. The stress analysis of inclusion problems of various shapes in an infinite anisotropic elastic medium was carried out. Antiplane study on confocal elliptical inhomogeneity problem using an alternating technique was carried out [8]. For the multi-inclusion problem under antiplane shears, dual null-field integral equation was suggested [9].

Faber series method for plane problems of an arbitrarily shaped inclusion was suggested [10]. The internal stress field of a three-phase elliptical inclusion was considered [11]. The inclusions are bonded to an infinite matrix through an interphase layer when the matrix is subjected to remote uniform stresses. The stress state for the three-phase composite with an inclusion of arbitrary shape was studied [12]. In the formulation, three phases take different elastic constant. Transfer matrix method is used for the solution of multiple elliptic layers with different elastic properties [13].

In this paper, the stress solution of for a square notch with small round corners is studied. The square notch is composed of two portions, or the matrix and the inclusion. The elastic property of the matrix portion is different to that of the inclusion. Remote loading is applied. Complex variable function method is used to solve the problem. The continuation conditions for traction and displacement along interface are formulated. Those conditions are satisfied in the sense of least residue. Therefore, the final solution will be evaluated from weight residue technique. The continuation condition for stresses along interface is examined. The stress concentration factors are evaluated.

2. Analysis

The solution of dissimilar inclusion problem for square notch with small round corners with remote loading are investigated in this paper (Figure1). In the matrix side, two elastic constants are denoted by G_1 , κ_1, and inclusion side by G_2 , κ_2 with $\kappa_2 = \kappa_1$. The remote loadings are denoted by σ_x^∞ , σ_y^∞ .

The following analysis depends on the complex variable function method in plane elasticity [1]. In the method, the stresses ($\sigma_x, \sigma_y, \sigma_{xy}$), the resultant forces (X, Y) and the displacements (u, v) are expressed in terms of two complex potentials $\phi(z)$ and $\psi(z)$ such that

$$\sigma_x + \sigma_y = 4\,\mathrm{Re}\,\phi'(z)$$

$$\sigma_y - \sigma_x + 2i\sigma_{xy} = 2[\bar{z}\phi''(z) + \psi'(z)] \tag{1}$$

$$F = -Y + iX = \phi(z) + z\overline{\phi'(z)} + \overline{\psi(z)} \tag{2}$$

$$2G(u+iv)=\kappa\phi(z)-z\overline{\phi'(z)}-\overline{\psi(z)} \tag{3}$$

where z=x+iy denotes complex variable, G is the shear modulus of elasticity, $\kappa=(3-\nu)/(1+\nu)$ is for the plane stress problems, $\kappa=3-4\nu$ is for the plane strain problems, and ν is the Poisson's ratio. In the present study, the plane strain condition is assumed thoroughly.

In the analysis, we use the following conformal mapping for the square notch configuration (Figure 1) [1]

$$z=\omega(\varsigma)=\varsigma-\frac{1}{6\varsigma^3},\quad \omega'(\varsigma)=1+\frac{1}{2\varsigma^4} \tag{4}$$

which maps the infinite region exterior to the square notch contour Σ (in the z-plane) into exterior region of unite circle Λ (in the ς -plane) (Figure 1).

In addition to the analytic function $\omega(\varsigma)$, we can define the following analytic function [1]

$$\omega_1(\varsigma)=\overline{\omega}(\frac{1}{\varsigma})=\overline{\omega(\frac{1}{\overline{\varsigma}})}=-\frac{1}{6}\varsigma^3+\frac{1}{\varsigma} \tag{5}$$

Clearly, along the unit circle in the ς -plane with the relation $\overline{\varsigma}=1/\varsigma$, we have the following property

$$z=\omega(\varsigma)=\overline{\omega_1(\varsigma)}\ ,\quad \text{or}\quad \overline{z}=\omega_1(\varsigma)=\overline{\omega(\varsigma)}\ ,\quad (\text{for}\,\varsigma\in\Lambda) \tag{6}$$

Two complex potentials $\phi_{1o^*}(z)$, $\psi_{1o^*}(z)$ are assumed for the matrix portion, and other two complex potentials $\phi_{2o}(z)$, $\psi_{2o}(z)$ are assumed for the inclusion portion (Figure 1).

From Eqs. (2) and (3), the displacement and traction continuation conditions along the interface can be expressed as follows

$$\overline{\phi_{1o^*}(z)}+\overline{z}\phi'_{1o^*}(z)+\psi_{1o^*}(z)=\overline{\phi_{2o}(z)}+\overline{z}\phi'_{2o}(z)+\psi_{2o}(z),\ (z\in\Sigma) \tag{7}$$

$$G_2\{\kappa_1\overline{\phi_{1o^*}(z)}-(\overline{z}\phi'_{1o^*}(z)+\psi_{1o^*}(z))\}=G_1\{\kappa_2\overline{\phi_{2o}(z)}-(\overline{z}\phi'_{2o}(z)+\psi_{2o}(z))\},(z\in\Sigma) \tag{8}$$

Two complex potentials in the matrix portion are assumed in the following form

$$\phi_{1o^*}(z)=\Gamma z+\phi_{1o}(z)\quad \psi_{1o^*}(z)=\Gamma_1 z+\psi_{1o}(z) \tag{9}$$

Where Γ and Γ_1 are defined by

$$\Gamma=\frac{\sigma_x^\infty+\sigma_y^\infty}{4},\quad \Gamma_1=\frac{\sigma_y^\infty-\sigma_x^\infty}{2} \tag{10}$$

For the inclusion side, we cannot use the conformal mapping, and two complex potentials are assumed in the following form

$$\phi_{2o}(z)=\sum_{k=1}^{N}c_k z^{(2k-1)},\ \psi_{20}(z)=\sum_{k=1}^{N}d_k z^{(2k-1)},\quad (z\in S^-) \tag{11}$$

Substituting Eqs. (9) and (11) into Eqs. (7) and (8) yields

$$\{\overline{\phi_{1o}(z)}+\overline{z}\phi'_{1o}(z)+\psi_{1o}(z)\}-\{\overline{\phi_{2o}(z)}+\overline{z}\phi'_{2o}(z)+\psi_{2o}(z)\}=-2\Gamma\overline{z}-\Gamma_1 z,\quad (z\in\Sigma) \tag{12}$$

$$G_2\{\kappa_1\overline{\phi_{1o}(z)}-(\overline{z}\phi'_{1o}(z)+\psi_{1o}(z))\}-G_1\{\kappa_2\overline{\phi_{2o}(z)}-(\overline{z}\phi'_{2o}(z)+\psi_{2o}(z))\}=-G_2\{(\kappa_1-1)\Gamma\overline{z}-\Gamma_1 z\},\quad (z\in\Sigma) \tag{13}$$

In the eigenstrain problem, similar interface formulation can be found from [13].

In the matrix side, the following complex potentials are defined

$$\phi_{1o}(z)\Big|_{z=\omega(\varsigma)}=\phi_1(\varsigma)=\sum_{k=1}^{N}a_k\varsigma^{-(2k-1)},\ \psi_{1o}(z)\Big|_{z=\omega(\varsigma)}=\psi_1(\varsigma)=\sum_{k=1}^{N}b_k\varsigma^{-(2k-1)},\quad (\varsigma\in S_*^+) \tag{14}$$

By using Eq. (14), Eqs. (12) and (13) can be rewritten as

$$\{\overline{\phi_1(\varsigma)} + \frac{\omega_1(\varsigma)\phi_1'(\varsigma)}{\omega'(\varsigma)} + \psi_1(\varsigma)\} - \{\overline{\phi_{2o}(z)} + \bar{z}\phi_{2o}'(z) + \psi_{2o}(z)\} =$$

$$= -2\Gamma\bar{z} - \Gamma_1 z, \quad (z \in \Sigma \text{ , or } \varsigma \in \Lambda) \tag{15}$$

$$G_2\{\kappa_1\overline{\phi_1(\varsigma)} - (\frac{\omega_1(\varsigma)\phi_1'(\varsigma)}{\omega'(\varsigma)} + \psi_1(\varsigma))\} - G_1\{\kappa_2\overline{\phi_{2o}(z)} - (\bar{z}\phi_{2o}'(z) + \psi_{2o}(z))\} =$$

$$= -G_2\{(\kappa_1 - 1)\Gamma\bar{z} - \Gamma_1 z\}, \quad (z \in \Sigma \text{ , or } \varsigma \in \Lambda)) \tag{16}$$

We may take the following integral operator (using the result $d\varsigma = de^{i\theta} = i\varsigma d\theta$)

$$I = \frac{1}{2\pi i}\int_\Lambda \{...\}\varsigma^j \, d\varsigma \text{ , or } \quad I = \frac{1}{2\pi}\int_\Lambda \{...\}\varsigma^{j+1} d\theta \tag{17ab}$$

to both sides of Eq. (15) and (16).

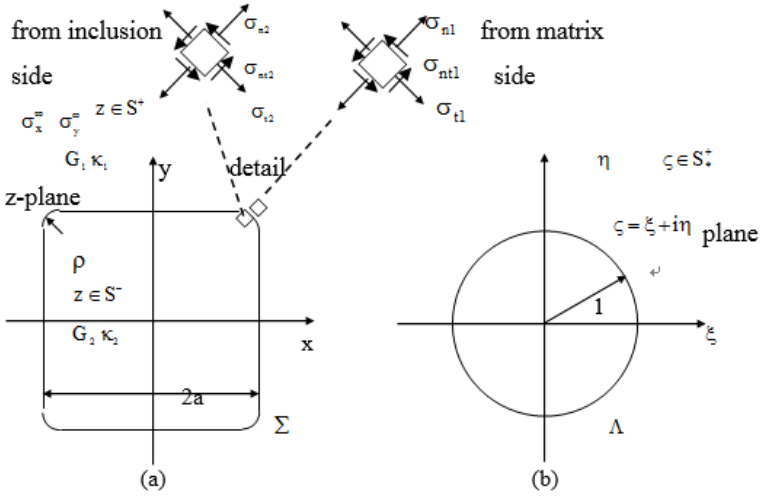

Figure 1. The loading and mapping relation for a square notch with small round corners (a) the loading condition and the material property in the formulation, (b) the unit circle configuration in the $\varsigma = \xi + i\eta$ plane

In the following particular case, we have

$$I = \frac{1}{2\pi i}\int_\Lambda \varsigma^j d\varsigma = \delta_j \text{ (with definition } \delta_j = 1, \text{ if } j = -1, \text{ and } \delta_j = 0, \text{ if } j \neq -1) \tag{18}$$

For some cases in Eq. (17ab), for example, the integrand $\{...\}$ take the following form, $\{...\} = \overline{\phi_{2o}(z)} = \sum_{k=1}^{N} c_k \bar{z}^{(2k-1)}$, or $\{...\} = \psi_{20}(z) = \sum_{k=1}^{N} d_k z^{(2k-1)}$, where z must be changed by $\omega(\varsigma)$. and $\bar{z}$ by $\omega_1(\varsigma)$ referred to Eqs. (4) and (5). In those integrands, the highest one is ς^{6N-3}, and lowest is $\varsigma^{-(6N-3)}$. Simply for finding the role of term ς^{6N-3} in the integration shown by Eq. (17ab), we can choose j=-6N+2 (note 6N-3-6N+2=-1). Similarly, for finding the role of ς^{-6N+3} in the integration shown by Eq. (17ab), we can choose j=6N-4 (note -6N+3+6N-4=-1). In conclusion, we need to use the integral operator shown by Eq. (17ab), from j=-6N+2. -6N+4, -6N+6,…..to 6N-4. The total amount for using integral operator is 6N-2 times.

For some cases in Eq. (17ab), for example, the integrand $\{...\}$ take the following form, $\{...\} = \overline{\phi_{2o}(z)} = \sum_{k=1}^{N} c_k \bar{z}^{(2k-1)}$, or $\{...\} = \psi_{20}(z) = \sum_{k=1}^{N} d_k z^{(2k-1)}$, where z must be changed by $\omega(\varsigma)$ .and $\bar{z}$ by $\omega_1(\varsigma)$ referred to Eqs. (4) and (5). In those integrands, the highest one is ς^{6N-3}, and lowest is $\varsigma^{-(6N-3)}$. Simply for

finding the role of term ς^{6N-3} in the integration shown by Eq. (17ab), we can choose j=-6N+2 (note 6N-3-6N+2=-1). Similarly, for finding the role of ς^{-6N+3} in the integration shown by Eq. (17ab), we can choose j=6N-4 (note -6N+3+6N-4=-1). In conclusion, we need to use the integral operator shown by Eq. (17ab), from j=-6N+2. -6N+4, -6N+6,…..to 6N-4. The total amount for using integral operator is 6N-2 times.

When performing the integral operator $I = \frac{1}{2\pi i}\int_{\Lambda} \{...\}\varsigma^{j}\, d\varsigma$, or $I = \frac{1}{2\pi}\int_{\Lambda} \{...\}\varsigma^{j+1} d\theta$ shown by (17ab) to Eq. (15) and (16), in some simple case, for example, if $\{...\} = \{\varsigma^{m}\}$, we can use Eq. (18). Otherwise, we have to use the numerical integration technique. Similar formulation for the use of the integral operator $I = \frac{1}{2\pi i}\int_{\Lambda} \{...\}\varsigma^{j}\, d\varsigma$ can be found in [13].

After using 6N-2 times of integration shown by Eq. (17ab) to both sides of Eqs. (15) and (16), we will obtain the following algebraic equation.

$$[Q]_{(12N-4)\times 4N}\ \{f\}_{4N} = \{g\}_{12N-4} \tag{19}$$

where $[Q]_{(12N-4)\times 4N}$ represents the matrix in the algebraic equation derived from left hand terms in Eqs. (15) and (16), $\{g\}_{12N-4}$ represents the vector in the algebraic equation derived from right hand terms in Eqs. (15) and (16). In Eq. (19), the following vector $\{f\}_{4N}$ is defined by

$$\{f\}_{4N} = \{a_1, a_2...a_N,\ b_1, b_2...b_N,\ c_1, c_2...c_N,\ d_1, d_2...d_N\}^{T} \tag{20}$$

which represents the unknowns in the studied problem.

In the derivation, because the number of equations (=12N-4) is larger than the number of unknowns (=4N), the algebraic equation shown by Eq. (19) cannot be satisfied exactly. Therefore, Eq. (19) is satisfied and solved in the sense of minimum of weight residue, which can be referred to [14].

After the vector $\{f\}_{4N} = \{a_1, a_2...a_N,\ b_1, b_2...b_N,\ c_1, c_2...c_N,\ d_1, d_2...d_N\}^{T}$ is evaluated by using the least square technique, the stress field of the matrix side and the inclusion side can be evaluated from Eq. (1).

In addition, if direction cosine to the contour Σ is denoted by $(\cos\beta\ \sin\beta)$ (Figure1), the stress components σ_n, σ_t and σ_{nt} can be evaluated by

$$\sigma_n = \sigma_x \cos^2\beta + \sigma_y \sin^2\beta + 2\sigma_{xy}\sin\beta\cos\beta,\quad \sigma_t = \sigma_x \sin^2\beta + \sigma_y \cos^2\beta - 2\sigma_{xy}\sin\beta\cos\beta$$

$$\sigma_{nt} = (-\sigma_x + \sigma_y)\sin\beta\cos\beta + \sigma_{xy}(\cos^2\beta - \sin^2\beta) \tag{21}$$

So far the theoretical derivation is completed.

2. Numerical examples

Four numerical examples are presented below. In all four examples, for the elastic constant, we choose $G_1 = 1$ and $\kappa_1 = \kappa_2 = 1.8$. In the first, second and third and fourth example, it is assumed $G_2 = 0.2$, $G_2 = 0.5$, $G_2 = 2$ and $G_2 = 5$ respectively. The assumed remote loading is denoted by $\sigma_x^* = \sigma_y^* = p$. N=12 terms are truncated in series expansion for complex potential.

Example 1

In the first example, the case for two phases is considered (Figure 1). It is assumed G_2 =0.2 in the first example. This is the soft inclusion case.

The stress solution along the interface from matrix side at $z = \omega(\varsigma)$ with $\varsigma = e^{i\theta}$ is denoted by

$$\sigma_{n1} = g_{n1}(\theta)p,\ \sigma_{t1} = g_{t1}(\theta)p,\ \sigma_{nt1} = g_{nt1}(\theta)p \quad \text{(from matrix side along interface)} \tag{22}$$

where $\sigma_x^{\infty} = \sigma_y^{\infty} = p$.

Secondly, in the case of $\kappa_1 = \kappa_2$, from Eq. (13) we see that the final solution solely depends on the ratio G_2 / G_1. In this case, two options (a) $G_1 = 1 kg/cm^2, G_2 = 0.2 kg/cm^2$, or (b) $G_1 = 1$, $G_2 = 0.2$, will give the same final solution.

There was a theorem in [1&44]. It was said in the theorem, if the tractions along the contour of matrix is in equilibrium, the solution for stresses at the matrix portion does not depend on the elastic constant. Therefore, for example the stress component along the interface can be expressed in the form $\sigma_{n1} = g_{n1}(\theta)p$ ($p = \sigma_x^{\infty} = \sigma_y^{\infty}$).

In addition, the stress solution along the interface from inclusion side at $z = \omega(\varsigma)$ with $\varsigma = e^{i\theta}$ is denoted by

$$\sigma_{n2} = g_{n2}(\theta)p\,,\sigma_{t2} = g_{t2}(\theta)p\,,\ \sigma_{nt2} = g_{nt2}(\theta)p \quad \text{(from inclusion side along interface)} \tag{23}$$

The computed results are plotted in Figure 2.

From Figure 2, it is seen that the condition $g_{n1}(\theta) = g_{n2}(\theta)$ and $g_{nt1}(\theta) = g_{nt2}(\theta)$ are almost satisfied. The $g_{t1}(\theta)$ value researches its maximum 2.71288 at the point $\theta = 45^{\circ}$, and $g_{t2}(\theta)$ value researches its minimum 0.16618 at the point $\theta = 45^{\circ}$. It is known that, if $G_2 = 0$, we have $g_{t1}(\theta)\big|_{\theta=45^{\circ}}$ =6 [14]. That is to say, the stress concentration factor is reduced to 45.21%.

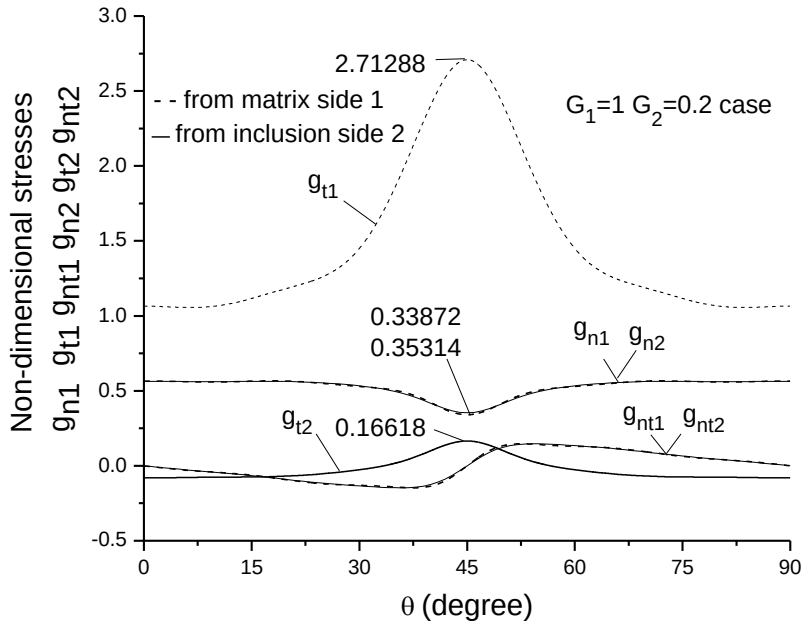

Figure 2. Non-dimensional stresses $g_{n1}(\theta)$, $g_{t1}(\theta)$, $g_{nt1}(\theta)$ from matrix side, and $g_{n2}(\theta)$, $g_{t2}(\theta)$, $g_{nt2}(\theta)$ from inclusion side along the interface in the case of $G_1 = 1$ $G_2 = 0.2$ [see Figure 1 and Eqs. (22) and (23)].

Example 2

In the second example, the case for two phases is considered (Figure 1). It is assumed G_2 =0.5 in the second example. This is the soft inclusion case. Same notations shown by Eqs. (22) and (23) are still used in this example. The computed results are plotted in Figure 3.

From Figure 3, it is seen that the condition $g_{n1}(\theta) = g_{n2}(\theta)$ and $g_{nt1}(\theta) = g_{nt2}(\theta)$ are almost satisfied. The $g_{t1}(\theta)$ value research its maximum 1.51337 at the point $\theta = 45^{\circ}$, and $g_{t2}(\theta)$ value research its minimum 0.11331 at the point $\theta = 45^{\circ}$. It is known that, if $G_2 = 0$, we have $g_{t1}(\theta)\big|_{\theta=45^{\circ}}$ =6. That is to say, the stress concentration factor is reduced to 25.22%.

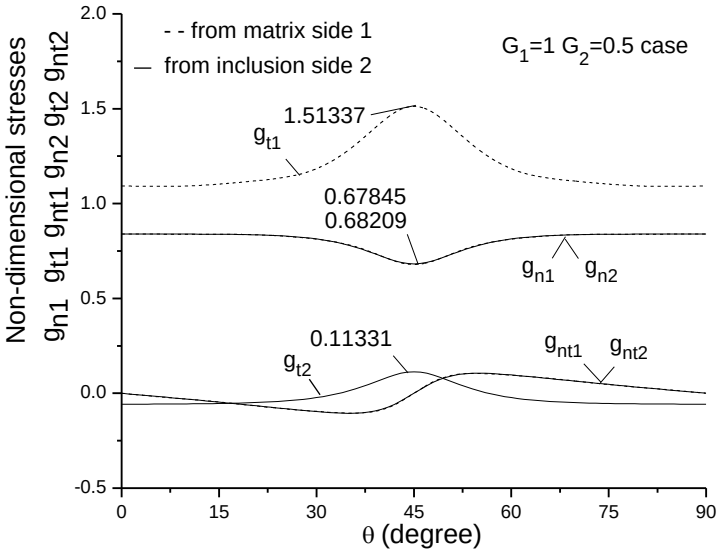

Figure 3. Non-dimensional stresses $g_{n1}(\theta)$, $g_{t1}(\theta)$, $g_{nt1}(\theta)$ from matrix side, and $g_{n2}(\theta)$, $g_{t2}(\theta)$, $g_{nt2}(\theta)$ from inclusion side along the interface in the case of $G_1 = 1$ $G_2 = 0.5$ [see Figure 1 and Eqs. (22) and (23)].

Example 3

In the third example, the case for two phases is considered (Figure 1). It is assumed G_2 =2 in the second example. This is the rigid inclusion case. Same notations shown by Eqs. (22) and (23) are still used in this example. The computed results are plotted in Figure 4.

From Figure 4, it is seen that the condition $g_{n1}(\theta) = g_{n2}(\theta)$ and $g_{nt1}(\theta) = g_{nt2}(\theta)$ are almost satisfied. The $g_{t1}(\theta)$ value research its maximum 0.80088 at the point $\theta = 45^o$, and $g_{t2}(\theta)$ value research its minimum -0.14176 at the point $\theta = 45^o$. It is known that, if $G_2 = 0$, we have $g_{t1}(\theta)\big|_{\theta=45^o}$ =6. That is to say, the stress concentration factor is reduced to 13.35%.

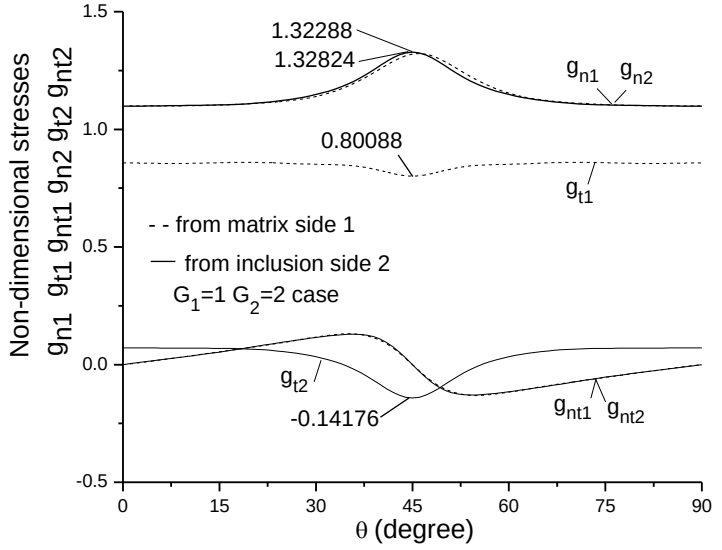

Figure 4. Non-dimensional stresses $g_{n1}(\theta)$, $g_{t1}(\theta)$, $g_{nt1}(\theta)$ from matrix side, and $g_{n2}(\theta)$, $g_{t2}(\theta)$, $g_{nt2}(\theta)$ from inclusion side along the interface in the case of $G_1 = 1$, $G_2 = 2$ [see Figure 1 and Eqs. (22) and (23)]

Example 4

In the fourth example, the case for two phases is considered (Figure 1). It is assumed G_2 =5 in the second example. This is the rigid inclusion case. Same notations shown by Eqs. (22) and (23) are still used in this example. The computed results are plotted in Figure 5.

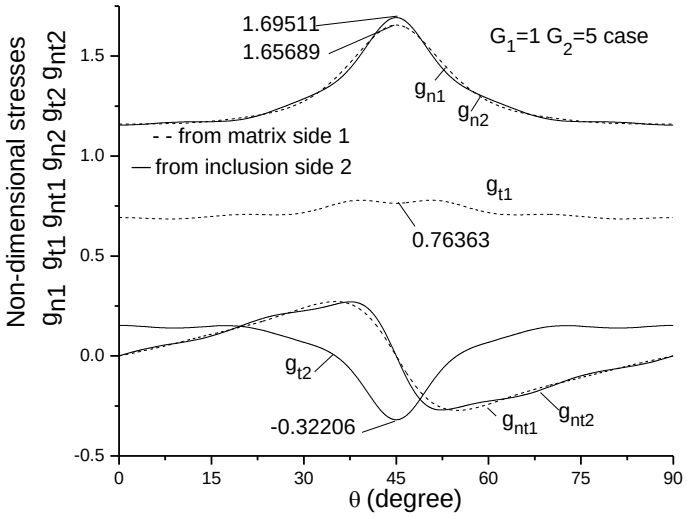

Figure 5. Non-dimensional stresses $g_{n1}(\theta)$, $g_{t1}(\theta)$, $g_{nt1}(\theta)$ from matrix side, and $g_{n2}(\theta)$, $g_{t2}(\theta)$, $g_{nt2}(\theta)$ from inclusion side along the interface in the case of $G_1 = 1$ $G_2 = 5$ [see Figure 1 and Eqs. (22) and (23)].

From Figure 5, it is seen that the condition $g_{n1}(\theta) = g_{n2}(\theta)$ and $g_{nt1}(\theta) = g_{nt2}(\theta)$ are almost satisfied. The $g_{t1}(\theta)$ value research its maximum 0.76363 at the point $\theta = 45^o$, and $g_{t2}(\theta)$ value research its minimum -0.32206 at the point $\theta = 45^o$. It is known that, if $G_2 = 0$, we have $g_{t1}(\theta)\big|_{\theta=45^o}$ =6. That is to say, the stress concentration factor is reduced to 12.73%.

3. Conclusions

The weight residue technique for the solution of dissimilar inclusion problem for square notch with small round corners in plane elasticity is suggested. A very accurate numerical technique for solving the square notch problem with small round corners was developed. This can be seen from $\sigma_{n1}(\theta) \approx \sigma_{n2}(\theta)$, $\sigma_{nt1}(\theta) \approx \sigma_{nt2}(\theta)$ (here, footnote 1- from matrix side, footnote 2- from inclusion side), which were plotted in Figures 2 to 5. Particularly, for a rigid inclusion case, for example, $G_2 = 5$, the relevant stress concentration factor can be reduced to 12.73%.

For the inclusion with arbitrary configuration, there is no effective technique to solve the dissimilar inclusion problem. Probably, the boundary integration equation method is way to solve the problem.

Declaration of Competing Interest: None.

References

[1] N.I. Muskhelishvili, Some Basic Problems of Mathematical Theory of Elasticity, Noordhoof, Groningen, 1963.
[2] S.N. Savin, Stress Distribution around Notches (English translation edition), Pergamon Press, Oxford, 1961.
[3] T. Mura, Micromechanics of Defects in Solids, Second ed. Martinus Nijhoff, Dordrecht, Netherlands, 1987.
[4] K. Zhou, H.J. Hoh, X. Wang, L.M. Keer, J.H.L. Pang, B. Song, Q.J. Wang, A review of recent works on inclusions, Mech. Mater. 60 (2013) 144-158.
[5] X.Q. Jin, Z.J. Wang, Q.H. Zhou, L.M. Keer, Q. Wang, On the solution of an elliptical inhomogeneity in plane elasticity by the equivalent inclusion method, J. Elast. 114 (2014) 1–18.
[6] C.S. Chang, H.D. Conway, Stress analysis of an infinite plate containing an elastic rectangular inclusion, Acta Mech. 8 (1969)160-173.
[7] C.Y. Dong, S.H. Lo, Y.K. Cheung, Stress analysis of inclusion problems of various shapes in an infinite anisotropic elastic medium, Comput. Methods Appl. Mech. Engrg. 192 (2003) 683–696.
[8] M.H. Shen,· S.N. Chen,· F.M. Chen, Antiplane study on confocally elliptical inhomogeneity problem using an alternating technique, Arch. Appl. Mech. 75 (2016) 302–314.
[9] J. T. Chen, A. C. Wu, Null-field approach for the multi-inclusion problem under antiplane shears, ASME J. Appl. 74 (2007) 469-487.

[10] J. C. Luo, C. F. Gao, Faber series method for plane problems of an arbitrarily shaped inclusion, Acta Mech. 208 (2009) 133–145.
[11] X. Wang, Three-phase elliptical inclusions with internal uniform hydrostatic stresses in finite plane elastostatics, Acta Mech. 219 (2011) 77-90.
[12] X. Wang, X.L. Gao, On the uniform stress state inside an inclusion of arbitrary shape in a three-phase composite, Z. Angew. Math. Phys. 62 (2011) 1101–1116.

[13] Y.Z. Chen, Transfer matrix method for the solution of multiple elliptic layers with different elastic properties, Part. 1. Acta Mech. 226 (2015) 191-229.
[14] Y.Z. Chen, Solution for square notch problem with small round corners in plane elasticity under remote loading, Arch. Appl. Mech. 2021; 91: 2943-2947.